1. **Rasha yasen Abed, 2. Ghassan Abdullah Salman, 3. Nesrallh Salman**

Department of Power and Electrical Machones, College of Engineering, University of Diyala, Uraq

Voltage Collapse Study of Power System under Load Shedding Point

Abstract. The phenomenon of overloading has become a serious threat to the reliability of power delivery, especially in operating sectors of electrical power networks it leads to voltage collapses. Therefore, adjusting the link between voltage stability and loading need a clear indicator. In this paper a simplified method of presenting the voltage stability margin as a tool to assign the maximum loading of every loading node in the power network. The proposed method is based only on network data and bus voltage magnitude measurement. Considerable results of maximum loading edges are obtained where the weakest node of the power network is also indicated. To improve the voltage stability margin, a wind power generator (Doubly Fed Induction Generator - DFIG) is injected at the weakest node in the electric grid (11-Bus test system). As a result, when a wind power generator (DFIG) is used, the system voltages will improve, losses will decrease, and the system's ability to withstand the overload will increase.

Streszczenie. Zjawisko przeciążeń stało się poważnym zagrożeniem dla niezawodności dostaw energii elektrycznej, zwłaszcza w eksploatowanych odcinkach sieci elektroenergetycznych prowadzi do załamań napięcia. Dlatego dostosowanie związku między stabilnością napięcia a obciążeniem wymaga jasnego wskaźnika. W artykule przedstawiono uproszczoną metodę prezentacji marginesu stabilności napięciowej jako narzędzia do wyznaczania maksymalnego obciążenia każdego węzła obciążającego w sieci elektroenergetycznej. Zaproponowana metoda opiera się wyłącznie na danych sieciowych i pomiarze wielkości napięcia magistrali. Znaczące wyniki maksymalnych krawędzi obciążenia uzyskuje się tam, gdzie wskazany jest również najsłabszy węzeł sieci elektroenergetycznej. Aby poprawić margines stabilności napięcia, generator energii wiatrowej (Doubly Fed Induction Generator - DFIG) jest wtryskiwany do najsłabszego węzła sieci elektrycznej (system testowy 11-Bus). W rezultacie, gdy używany jest generator energii wiatrowej (DFIG), napięcia w systemie poprawią się, straty zmniejszą się, a zdolność systemu do wytrzymania przeciążenia wzrośnie. (Badanie zaniku napięcia w systemie elektroenergetycznym w punkcie zrzutu obciążenia)

Keywords: Voltage collapse, Voltage stability margin, Load shedding, wind Generator, DFIG
Słowa kluczowe: Spadek napięcia, margines stabilności napięcia, zrzut obciążenia, podwójnie zasilany generator indukcyjny
.

Introduction

The Excessive demand with limited resources certainly leads power system to the voltage collapse point or maximum power loading. The consumption of reactive power without local compensation may cause a speedily voltage magnitude decreases and line losses. In other ways the voltage collapse may occur during the deterioration of the voltage profile due to the increasing demand for reactive power in remote areas or buses. Voltage instability or voltage collapse can be considered the biggest problem that is usually connected to the stressed power system. The mentioned problems may lead to cause maloperation for steady-state conditions. One of the necessary things is estimating and knowing the maximum load that the network can provide. The load estimation depends on several factors, where voltage drop is one of them. The insufficient compensation of the reactive power to meet local demand and increased losses would lead to a decrease and deterioration of voltage, especially in remote areas [1, 2, 3]. A rapid decrease in the bus voltage will occur when the power system load just exceeds its maximum limit. However, the amount of voltage may not have been an acceptable indicator for defining the voltage [4, 5]. Voltage collapse is a reasonable tool to determine the maximum permissible load within the limits of voltage stability. It is one of the most important matters in the planning and operation of the power system. The PV and QV curves are frequently used for evaluating and determining voltage stability and maximum permissible load [1, 6]. It can be created by using multiple simulations of load flow [7,8,9]. It can be reached by calculating the extreme of load given bus under the assumption of remaining constant load for other buses. However, it isn't a very reasonable assumption. Furthermore, the assigned system which to estimate the bus's maximum loading may not accurately represent the original system with its entire operational range. There are many methods, such as the multiple load flow method [10], energy methods [11], singular value decomposition (SVD) [12], and Bifurcation theory [13], etc. have been published in the literature for analyzing voltage stability or establishing a system's maximum permitted loading. All of the approaches outlined above need a significant amount of calculation and so are not suitable for online use. References [14, 15] offer a new technique for enhancing voltage stability in power systems by employing PSO adaptive GSA hybrid algorithm and PSO algorithms to define the optimally size and location of FACTS devices. Reference [16] proposes strategies for FACTS element position and rating optimization by using the weighted coefficients and the Strength Paretto Evolutionary Algorithm (SPEA). A model can be applied to a single and double-cages description of the DFIG [17]. Voltage stability can be improved by using a DFIG wind turbine's reactive power output control capability [18]. To find the optimal location of (DFIG) and SVCs as well as the best injection of the reactive power to improve the voltage profile and loading level in the network [19].

In this paper, a simplified method of indicating the maximum loading of every bus bar in the power system is proposed. It is based only on power system data and bus voltage magnitude measurement. By this method, the weakest bus of the power network could be assigned, and then the wind power generator (DFIG) is added at the weakest bus bar of a power system to enhance the overall system performance (improve voltage profiles, decrease active and reactive power losses, and increase the system's ability to withstand the overload).

Section 2 provides a modeling formulation of the power system based on the Thevenin theorem. Section 3 describes the indicator of the voltage stability margin of the power systems. Section 4 presents the proposed model of a wind generator (DFIG) to prevent voltage collapse. Section 5 discussed the simulation results used to evaluate the performance of the proposed method (VSM and DFIG) using the 11-Bus system. Section 6 draws conclusions.

Power System Modeling

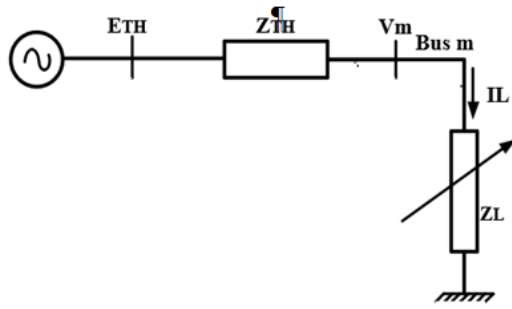Suppose a bus m with a load as $S_m = P_m + jQ_m$ supplied by a typical power system as in Figure 1[3].

Fig 1. Impersonation of load bus m in general power system.

Fig 2. Boundary Voltage Stability [20].

Typically, any part of power system may consist of numbers of loads, transmission lines and generators. When Thevenin equivalent applied to this part of power system, the system become simply 2 buses (Figure 1) to find Thevenin equivalent parameters E_{TH} and Z_{TH} by measuring bus voltage on-line under different load situations, the load impedance Z_L can be formulated as:

$$(1) \qquad Z_{L=}\frac{V_m^2}{S_m^*}$$

The magnitude of the voltage on bus m is V_m, and apparent power load is S_m^*,

$$(2) \qquad S_m = \frac{E_{Th}^2 Z_L}{Z_{Th}^2 + Z_L^2 + 2Z_{Th}Z_L \cos(\beta-\theta)}$$

where

$Z_{Th}=Z_{Th}\angle\beta =(R_{Th} + jX_{Th}), Z_L=Z_L\angle 0 =(R_L + jX_L)$

$E_{Th}=E_{Th}\angle\delta =(E_{Thre} + jE_{Thim})$

$S_m=S_m\angle 0 =(P_m + jQ_m)$

Meanwhile, the apparent power of maximum load can be expressed as:

$$(3) \qquad \frac{\partial S_m}{\partial Z_L} = 0$$

equation (3) provides

$$(4) \qquad Z_L = Z_{Th}$$

The voltage collapse occurs when the loading impedance magnitude is equal to Thevenin impedance magnitude and maximum loading occurs. by using equation (4) in (2) critical apparent power of bus load m equal:

$$(5) \qquad S_m^{CY} = \frac{E_{Th}^2}{2Z_{Th}[1+\cos(\beta-\theta)]}$$

Equation (5) demonstrates that the parameters of the Thevennen model are the main elements of maximum loading expression. However, the mentioned factors are not always constant. As a result, proper maximum loading calculation requires online surveillance of Thevenin parameters.

Voltage Stability Margin (VSM)
As previously stated, the system achieves its maximum load point when the following conditions are met:

$$(6) \qquad Z_L = Z_{Th} \rightarrow Y_L = Y_{Th}$$

As illustrated in Figure 2, stability of voltage barrier may be characterized through a circle of radius Y as Thevenin admittance meanwhile Y_L is the admittance of load that is contained within the circle. It indicates normal operation, where the system works on the typical P-V curve's upper portion (or stable area) [3, 4].
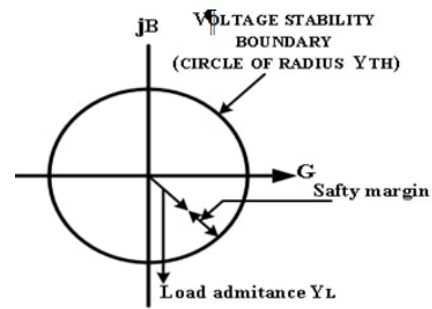
A voltage collapse occurs when Y_L, Y surpasses Y_{Th}, and the system runs in the lower portion of the P-V curve (or unstable area). Load admittance and Thevenin admittance are the same ($Y_L = Y_{TH}$) at the highest power point. Y_L is the load admittance for a given load. The distinction between Y_{TH} and Y_L may be thought of as a:

$$(7) \qquad VSM_y = \frac{Y_{Th} - Y_L}{Y_{Th}}$$

It is noted in the characterized circle shown in Figure 2 that the first and fourth quadrants represent capacitive and inductive loads operation behavior respectively. While, the operation is not possible in the second and third quadrants for a positive charge because of requirement of a negative charge conductivity G. The definition of voltage stability margin (VSM) in (7) is not an intuitive value. This margin is best expressed in terms of apparent load power (VSM$_s$). It can be written by using equation (2) and equation (5)

$$(8) \qquad VSM_S = \frac{(Z_L - Z_{Th})^2}{Z_{Th}^2 + Z_L^2 + 2Z_{Th}Z_L \cos(\beta-\theta)}$$

It can be noticed that both VSM_Y and VSM$_s$ are normalized amounts and reduce its values when the load increases. At the voltage breakdown point each margin lessens to 0 and the corresponding load is taken into consideration due to maximum permissible loading. It can be observed that the voltage drop point of the system reached when the bus current load m increases by a factor r_m. It means, r_m can be expressed as a ratio of the critical load and the current load:

$$(9) \qquad r^m = \frac{s_m^{cr}}{s_m}$$

The value of r_m may be expressed as follows using equation (2) and equation (5):

$$(10) \qquad r_m = 1 + \frac{(Z_L - Z_{Th})^2}{2Z_{Th}Z_L[1+\cos(\beta-\theta)]}$$

The critical or greatest permitted loading of bus m (S_m^{cr}) is estimated at current load of S_m is:

$$(11) \qquad S_m^{cr} = r_m S_m$$

The procedures described above for determining maximum permitted loading and voltage stability margins can be done to every load bus in the system. A vulnerability index of every load bus to voltage collapse can be indicated by the lowest value of VSM, where this bus is regarded as the weakest bus in the system.

The weakest bus indication is very useful in prediction of voltage collapse occurrence situation during the consistent load grown on a power system. Based on the mentioned procedure, at the critical point means at voltage collapse

point, the maximum permissible loading of the system (S_{sys}^{cr}) can be expressed as:

$$（12） \quad S_{sys}^{cr} = r'S_{SYS}$$

Where r' is the value of the load multiplier factor of the system's weakest bus determined by (11) at the current system load [20].

Wind Generator Modeling (DFIG)

Many large wind farms will use variable speed wind turbines powered by doubly fed induction generators (DFIG). It's used a wound rotor induction generator, which is fed by variable frequency, voltage source, and converters. The DFIG steady-state electrical equations are assumed because the stator and rotor flux dynamics are fast in comparison to grid dynamics and the converter controls effectively decouple the generator from the grid [21]. As a consequence of these presumptions, one has:

$$（13）\quad v_{ds} = -r_s i_{ds} + \left((x_s + x_m) i_{qs} + x_m i_{qr} \right)$$

$$（14）\quad v_{qs} = -r_s i_{qs} - \left((x_s + x_m) i_{ds} + x_m i_{dr} \right)$$

$$（15）\quad v_{dr} = -r_R i_{dr} + (1-w_m)\left((x_R + x_m) i_{qs} + x_m i_{qr} \right)$$

$$（16）\quad v_{qr} = -r_R i_{qr} + (1-w_m)\left((x_R + x_m) i_{ds} + x_m i_{ds} \right)$$

The voltages of stator depend on the amplitude and phase of the grid voltage:

$$（17）\quad v_{ds} = V\sin(-\theta)$$

$$（18）\quad v_{qs} = V\cos(\theta)$$

According to the following, the stator currents and grid side currents of the converter determine the active and reactive powers injected into the grid:

$$（19）\quad P = v_{ds}i_{ds} + v_{qs}i_{qs} + v_{dc}i_{dc} + v_{qc}i_{qc}$$

$$（20）\quad Q = v_{ds}i_{ds} - v_{ds}i_{qs} + v_{qc}i_{dc} - v_{dc}i_{qc}$$

As mentioned below, can be reformulated taking into account the converter power equations. The grid side converter powers are:

$$（21）\quad P_c = v_{dc}i_{dc} + v_{qc}i_{qc}$$

$$（22）\quad Q_c = v_{qc}i_{dc} - v_{dc}i_{qc}$$

However, on the side of the rotor:

$$（23）\quad P_r = v_{dr}i_{dr} - v_{qr}i_{qr}$$

$$（24）\quad Q_r = v_{qr}i_{dr} - v_{dr}i_{qr}$$

As a result, the power supplied to the grid produces:

$$（25）\quad P = v_{ds}i_{ds} + v_{qs}i_{qs} + v_{dr}i_{dr} + v_{qr}i_{qr}$$

$$（26）\quad Q = v_{qs}i_{ds} - v_{ds}i_{qs}$$

Result

The suggested approach for monitoring a power system's maximum allowable loads and voltage stability margins was tested on the 11-Bus network systems shown in Figure 3 [22].

The system has one slack busbar (Bus No.1), two P-V buses (Buses No.10 and No.11), and eight P-Q buses (Buses No.2 to No.9). The base of the system load is 1000 MVA. The system's load flow problems are conducted by evenly Load Increasing (LI) for P-Q buses of the system by (10%, 20%, 30%, 40%, and 50%). Under various loading conditions, there is a need for bus voltage values, which are obtained from the load flow analysis. The weakest buses in the system are determined based on equation (8).
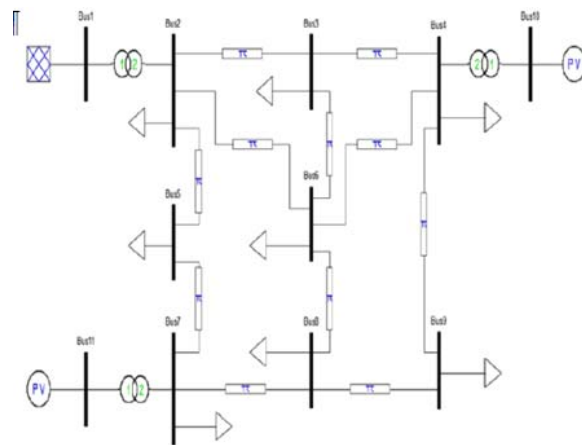

Fig 3. Model of the analyzed network (without DFIG).

Under Normal Loads (NL), the bus voltages range between 1.023 volts for bus 2 and 0.974 volts for bus 9. When busloads steadily rise from 10% to 50% by steps, a general drop in voltages is observed in the power system, with buses No.8 and No.9 voltage being most affected in comparison to their original voltage. In order to see these results graphically, shown in Figure 4.
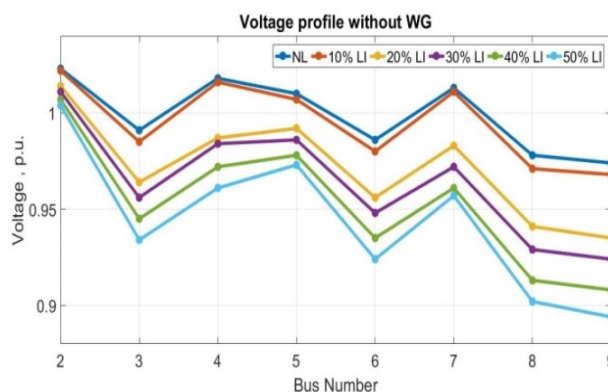

Fig 4. Voltage profile with load increase (without DFIG).

VSM is critical in studying voltage instability since it reveals how far the power system can operate before suffering voltage instability. The data listed in Table 1 shows the magnitude of VSM with increased load. It is observed from Table 1, when the loads are gradually increased that bus No.9 is the weakest bus in the system.

Table 1. VSM with load increased (without DFIG).

	NL	LI 10%	LI 20%	LI 30%	LI 40%	LI 50%
VSM Bus2	0.970	0.951	0.925	0.903	0.884	0.871
VSM Bus3	0.981	0.954	0.900	0.853	0.802	0.762
VSM Bus4	0.962	0.950	0.931	0.919	0.907	0.898
VSM Bus5	1.000	0.999	0.987	0.967	0.938	0.857
VSM Bus6	0.976	0.946	0.892	0.848	0.805	0.776
VSM Bus7	0.997	0.991	0.976	0.959	0.936	0.915
VSM Bus8	0.998	0.985	0.940	0.889	0.829	0.779
VSM Bus9	0.975	0.948	0.889	0.841	0.788	0.748

In order to improve the performance of the system, the Wind Generator (WG i.e. DFIG) is connected to the weakest bus, consequently, the DFIG connects on bus No.9

to treat the trouble of voltage drops on the buses caused by growing loads, Figure 5 shows the analyzed network with Wind Generator. The voltage of the buses has significantly increased, especially on buses No.9 and No.8. These are shown in Figure 6.
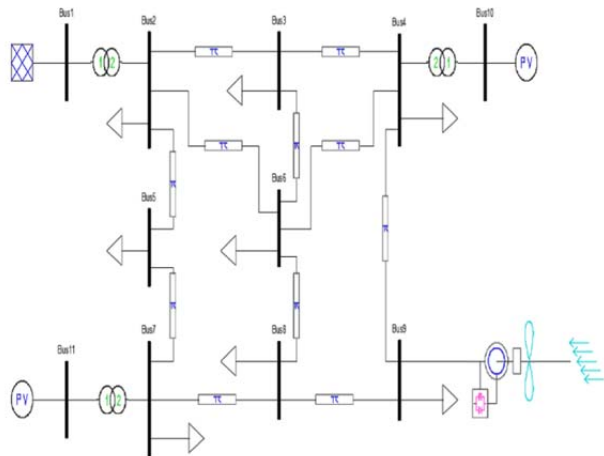

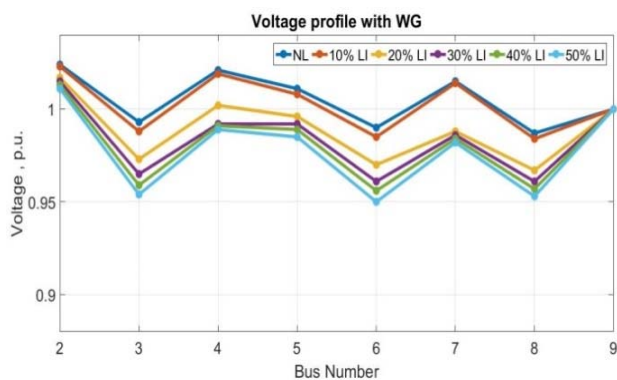Fig 5. Model of the analyzed network (with DFIG).

Fig 6. Voltage profile with load increase (with DFIG).

For making the comparison and demonstrating the effectiveness of adding a WG on voltage profiles, Figure 7 shows the case of NL with and without WG, and shows the case of a 50% load increase with and without WG.
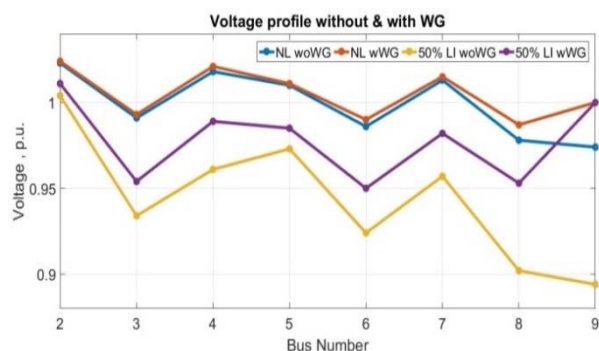

Fig 7. Voltage profile without and with Wind Generator.

As for the VSM indicator, after adding the DFIG to the analyzed network, all buses moved away from the voltage collapse point (although there is a gradual increase in loads) as shown in Table 2, and specifically bus No.9, it improved significantly.

For making the comparison and demonstrating the effectiveness of adding a WG on the VSM indicator (buses No.8 and No.9), The real power losses and the reactive

power losses in the transmission lines of the network (which consists of 14 transmission lines) with and without WG are shown in Figure 8 (P_{Losses}) and Figure 9 (Q_{Losses}). As the real power losses are reduced by 1.442 MW at NL, and the reactive power losses are reduced by 8.603 Mvar at NL.

Table 2. VSM with load increased (with DFIG).

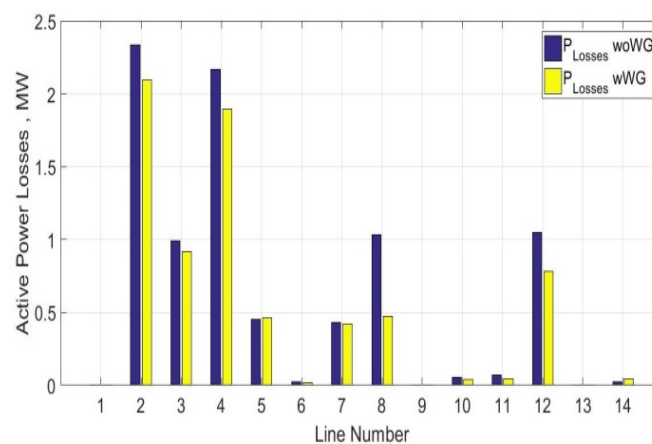|	NL	LI 10%	LI 20%	LI 30%	LI 40%	LI 50%
VSM Bus2	0.971	0.952	0.928	0.907	0.888	0.874
VSM Bus3	0.983	0.957	0.912	0.865	0.821	0.782
VSM Bus4	0.963	0.951	0.936	0.922	0.912	0.903
VSM Bus5	0.999	0.999	0.990	0.972	0.949	0.873
VSM Bus6	0.978	0.951	0.906	0.863	0.825	0.793
VSM Bus7	0.997	0.992	0.980	0.966	0.950	0.932
VSM Bus8	0.999	0.990	0.961	0.924	0.881	0.837
VSM Bus9	0.982	0.962	0.932	0.900	0.866	0.832

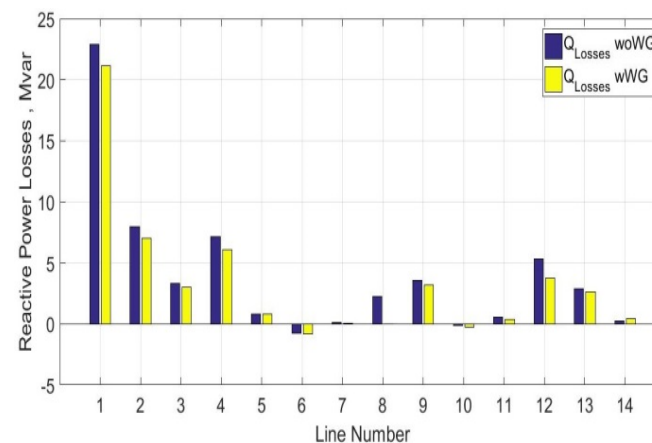Fig 8. P_{Losses} without and with Wind Generator.

Fig 9. Q_{Losses} without and with Wind Generator.

Conclusions

This study presents a very basic and uncomplicated approach for calculating the maximum allowable loads and voltage stability margin using data of power system. The offer process is capable for controling a correct value of maximum load, knowing the magnitude of the bus voltage, as well as the load power in both components real and reactive. The required data such as buses voltages and You can acquire load information either from the load flow simulation when planning the power system or from real-time measurements during the operation of power system.

The procedure accurately method the stressed system using data loading to constantly redevelop the extreme load and VSM values. Because the calculation needed in data processing is relatively basic, the suggested approach was simulated throughout the 11-Bus system to determine the extreme allowable load and VSM at different operational stages. From the obtained results, it is shown that the voltage index VSM is seveirly sensitive to load level. Its significant effect is at the verge of voltage breakdown. VSM, otherwise fluctuates virtually linear with the load level of the system. So it offers a superior indicator in terms of perceived power. the suggested technique may properly predict the maximum permitted loading at the voltage breakdown, where it is considered critical point. The proposed procedure is only utilizing information from the present operating point. The performance of the system, in general, has also been improved by adding Wind Generators (DFIG) to the already identified weakest bus in the power system using the VSM index. Based on the obtained results, important power system elements has been improved such as Voltage profile, reduction in real and reactive power losses, as well as the buses carrying capacity increased when overloaded (system buses decreased the incidence of voltage collapse point).

Authors: Rasha Yasen Abed E-mail: rashaabed876@gmail.com ; Ghassan Abdullah Salman, E-mail: ghassanpowerz@gmail.com; Nesrallh Salman, Email: dr.Nasrallah@engineering.uodiyala.edu.iq; Department of Power and Electrical Machines, College of Engineering University of Diyala, Baqubah, Iraq

REFRENCE

[1] Koessler,RodolfoJ. "Voltagein stability/collapse-an overview" *IEE Colloquium on Voltage Collapse* (Digest No: 1997/101). IET, 1997.
[2] Husham Idan Hussein, Hassan Saadallah Naji, Ghassan Abdullah Salman, "Voltage stability assessment prediction using a guide strategy-based adaptive particle swarm optimisation-neural network algorithm" *International Journal of Power Electronics and Drive Systems* (IJPEDS), Vol. 13, No. 4, December 2022, pp. 2199-2206.
[3] Ahmed Majeed Ghadban, Ghassan Abdullah Salman, Husham Idan Hussein," Assessment of voltage stability based on power transfer stability index using computational intelligence models" *International Journal of Electrical and Computer Engineering (IJECE),* Vol. 11, No. 4, August 2021, pp. 2790-2797.
[4] Clark, H. K. "New challenge: Voltage stability" *IEEE Power Engineering Review ;(USA)* (1990).
[5] Hatim G. Abood, Ghassan Abdullah Salman, and Ali Sachit Kaittan," A Regularized Approach for Solving Ill-Conditioned State Estimation of Distribution Systems" *ELEKTROTEHNIŠKI VESTNIK* 86(3): 137-143, 2019.
[6] Balu, C. W. T. N. J., and Dominic Maratukulam. " Power system voltage stability " New York, NY, USA: McGraw-Hill, 1994.
[7] Haque, Ml H. "A fast method for determining the voltage stability limit of a power system." *Electric power systems research* 32.1 (1995): 35-43.
[8] GUNADIN, Indar Chaerah, et al. "Forecasting Voltage Collapse when Large-Scale Wind Turbines Penetrated to Power Systems Using Optimally Pruned Extreme Learning Machines (OPELM)-Case Study: Electric Power System South Sulawesi-Indonesia." Przegląd Elektrotechniczny, ISSN 0033-2097, r. 98 nr 5/2022 (2022).
[9] Verayiah, Renuga, et al. "Review of under-voltage load shedding schemes in power system operation." Przegląd elektrotechniczny 90.7 (2014): 99-103.
[10] Salman, Nesrallh, Azah Mohamed, and Hussain Shareef. "Reliability improvement in distribution systems by optimal placement of DSTATCOM using binary gravitational search algorithm." Przegląd Elektrotechniczny 88.2 (2012): 295-299.
[11] Overbye, Thomas J., and Christopha L. DeMarco. "Improved techniques for power system voltage stability assessment using energy methods." *IEEE Transactions on Power Systems* 6.4 (1991): 1446-1452.
[12] Lof, P-A., et al. "Fast calculation of a voltage stability index." *IEEE Transactions on Power Systems* 7.1 (1992): 54-64.
[13] Canizares, Claudio A. "On bifurcations, voltage collapse and load modeling." *IEEE transactions on power systems* 10.1 (1995): 512-522.
[14] Inkollu, Sai Ram, and Venkata Reddy Kota. "Optimal setting of FACTS devices for voltage stability improvement using PSO adaptive GSA hybrid algorithm." *Engineering science and technology, an international journal* 19.3 (2016): 1166-1176.
[15] Ghassan Abdullah Salman, Hatim G. Abood, Mayyadah Sahib Ibrahim, "Improvement the voltage stability margin of Iraqi power system using the optimal values of FACTS devices", International Journal of Electrical and Computer Engineering (IJECE), Vol. 11, No. 2, April 2021, pp. 984-992.
[16] Kianersi, Hadi, and Hamid Asadi. "Voltage stability improvement by using FACTS elements with economic consideration." *Ciência e Natura* 37.6-2 (2015): 162-167.
[17] Ekanayake, Janaka B., et al. "Dynamic modeling of doubly fed induction generator wind turbines." *IEEE transactions on power systems* 18.2 (2003): 803-809.
[18] Zebar, Abdelkrim. "Static synchronous compensator and superconducting fault current limiter for power transmission system transient stability regulation including wind generator." Przegląd Elektrotechniczny 96 (2020).
[19] A. N. J. Almakki, "Using Feedback Control to Control Rotor Flux and Torque of the DFIG-Based Wind Power System, " International Journal of Engineering and Technology Innovation, vol. 13, no. 1, pp. 70-85 , 2023.
[20] Haque, M. H. "On-line monitoring of maximum permissible loading of a power system within voltage stability limits." *IEE Proceedings-Generation, Transmission and Distribution* 150.1 (2003): 107-112.
[21] Federico Milano. "Power System Analysis Toolbox." Documentation for PSAT version 1.3.4, July 14, 2005
[22] Sadat,Hadi."Power system analysis." *McGraw-Hill Inc* (1999).